Int. J. Appl. Math. and Comp. Sci., 1999, Vol.9, No.2, 327–346

STRUCTURAL FORMULATION AND SELF-OSCILLATION PREDICTION IN MULTIDIMENSIONAL NONLINEAR CLOSED-LOOP AUTONOMOUS SYSTEMS

KARTIK C. PATRA*, BIBHUTI B. PATI*, ADAM ŁOZOWICKI**

This paper describes the structure of a general two-dimensional nonlinear closed-loop system and application of the universal chart, leading to the use of computer graphics, for a systematic analysis of the complex problem of predicting self-oscillations (limit cycles). The graphical approach provides an explicit and novel insight into the conditions for the occurrence of limit cycles in such systems. This technique forms the basis of computer algorithms for predicting limit cycles in multidimensional nonlinear systems. Application of the technique has been illustrated through examples and comparison of results with digital simulation in MATLAB 4.0/SIMULINK 1.3.

Keywords: universal chart, phasor diagram, limit cycles, multidimensional, nonlinear system, describing function.

1. Introduction

Increasingly complex physical plants are commonly demanded in view of today's industrial needs. The control of those plants has become a problem due to both the plant complexity and attendant stringent control requirements. Such plants are usually characterised by multiple inputs, as well as multiple outputs. The outputs are physical variables over which some degree of control is to be exerted.

The plants under consideration may be mathematically described by parameters relating one set of plant variables to another. A particular parameter may represent a very small physical portion of the plant, yet for engineering reasons the identity of this parameter is important and should be retained in the design of a control system for the plant. For example, this parameter can be peculiarly subjected to variation in the response to an environmental disturbance. By retaining this parameter's explicit identity, the parameter variation can be accommodated to the control system specifications by feedback, adaptive or other techniques.

* Department of Electrical Engineering, Indira Gandhi Institute of Technology, SARANG, Orissa, India, PIN: 759–146.

** Technical University of Szczecin, Institute of Control Engineering, ul. Gen. Sikorskiego 37, 70–313 Szczecin, Poland, e-mail: lozowicki@ps.pl.

This structure technique based upon intermediate variables and parameters of the plant is discussed here for multivariable systems with interactions between individual systems. A systematic review of the nature and structure of nonlinear multivariable systems reveals the existence of many distinct structural forms (i.e. interconnection of the elements constituting the system) unlike linear systems (Singh, 1965). However, most of the work on nonlinear mutivariable systems continues to be developed in a general framework and, in general, little use is made of the character of the system structure in the analysis of symmetric self-oscillations (limit cycles), the *modus operandi* of nonlinear systems (Atherton, 1975; Atherton and Dorrah, 1980). The paper investigates the nature of possible system structures that a general two-dimensional system with nonlinear elements can possess. Subsequently, several important sub-classes of this general structure are obtained by successive simplifications. A large number of industrial systems like coupled core reactors (Raju and Josselson, 1971), PWR-type nuclear-reactor systems (Parlos *et al.*, 1988), radar antennae pointing systems (Nikiforuk and Wintonyk, 1968) are known to possess the structure of a two-dimensional nonlinear system.

Recognition of limit cycles, the *modus operandi* of nonlinear systems analysis, has had a long and glorious history. Although no truly significant results have been obtained in recent years for multidimensional systems, the study of limit cycle prediction is of evident importance and hence addressed in this work.

Unfortunately, in spite of a great amount of work, it is well-known that exact methods concerning limit cycle prediction are rare and even if they exist, they are difficult to apply. Thus approximate methods are used and probably the most versatile, especially for complex and higher-order systems, is the sinusoidal input describing function (DF) method. The describing-function approach provides a convenient tool to analyse such oscillations and, by virtue of its inherent approximations, leads to a significant reduction in the complexity of the analysis itself. A graphical technique suitable for computer graphics has been developed for prediction of limit cycles in two-input/two-output nonlinear systems. The paper presents a universal chart for limit-cycle prediction. To the authors' knowledge, this is the first work on limit-cycle prediction of two-dimensional systems using universal charts. The attractive features of the paper worth mentioning are as follows:

(i) A most general structure has been developed in view of the coupling effect between subsystems and claims more suitable for oscillation prediction. In addition, the chances are that any practical 2×2 system can be reduced to this general structure form. The authors would like to mention that from the limit-cycle point of view nothing is gained by complicating the situation by overemphasizing the importance of a structure which is different from that mentioned here.

(ii) Apart from a direct application, the method has the clear advantage that it brings out the influence of an individual system (the effect of interaction/coupling) on the oscillation parameter.

(iii) The paper depicts clearly the amplitude ratio condition derived from the cross-coupled MIMO system and has been used in conjunction with phase and gain conditions for determining a limit cycle.

(iv) The graphical technique (universal chart) forms a basis for computer algorithms of limit-cycle prediction.

(v) The technique is derived from the basic concept of phasor relationships between system variables and illustrated through examples without loss of generality.

(vi) The simplicity of the method and its close connection with frequency concepts explain its wide practical application.

Notation:

ω	Frequency [rad/s].
G	Linear element transfer function, function of frequency.
R_1, R_2	Amplitudes of inputs to Subsystems 1 and 2, respectively.
X_1, X_2	Amplitudes of inputs to nonlinearities.
Y_1, Y_2	Amplitudes of nonlinear element outputs.
C_1, C_2	Amplitudes of subsystem outputs.
N_1, N_2	Nonlinear functions of X_1 and X_2.
θ_c	Phase angle between C and R.
θ_L	Phase angle contributed by linear elements at a particular ω.

2. A Most General Two Dimensional Nonlinear System Configuration

This is an extension of the corresponding representation of a SISO system incorporating one nonlinear element developed in (Singh and Subramanian, 1980; Subramanian, 1978). To the best of our knowledge, this extension develops for the first time a general framework for two-dimensional systems in a systematic and rational manner.

Figure 1(a) shows a two-input/two-output system incorporating only two nonlinear elements and any number of linear elements connected in any arbitrary manner. Since the system incorporates only two nonlinear elements, it follows that, in the most general case, signals x_1, x_2, c_1 and c_2 must be derived from the signals u_1, u_2, x_1, x_2, y_1, y_2, c_1 and c_2 passing through appropriate linear transmittances as shown in Figs. 1(b)–(e). The signal flow graph (SFG) of the most general system can therefore be visualised as the union of Figs. 1(b)–(e) as shown in Fig. 2(a) which can be finally reduced to Fig. 2(b) or its equivalent block diagram representation as shown in Fig. 3.

The general system represented by Fig. 3 can further be simplified to the equivalent representation shown in Fig. 4. This is treated as the most general two-dimensional nonlinear system. From this structure, a special case shown in Fig. 5 is obtained for which $G_{11} = 1$ and the other linear transfer functions have been given new designations. Furthermore, from Fig. 5, an interesting case shown in Fig. 6 is obtained, where $G_3 = -1$. It can be noted that in the transformation from Fig. 3

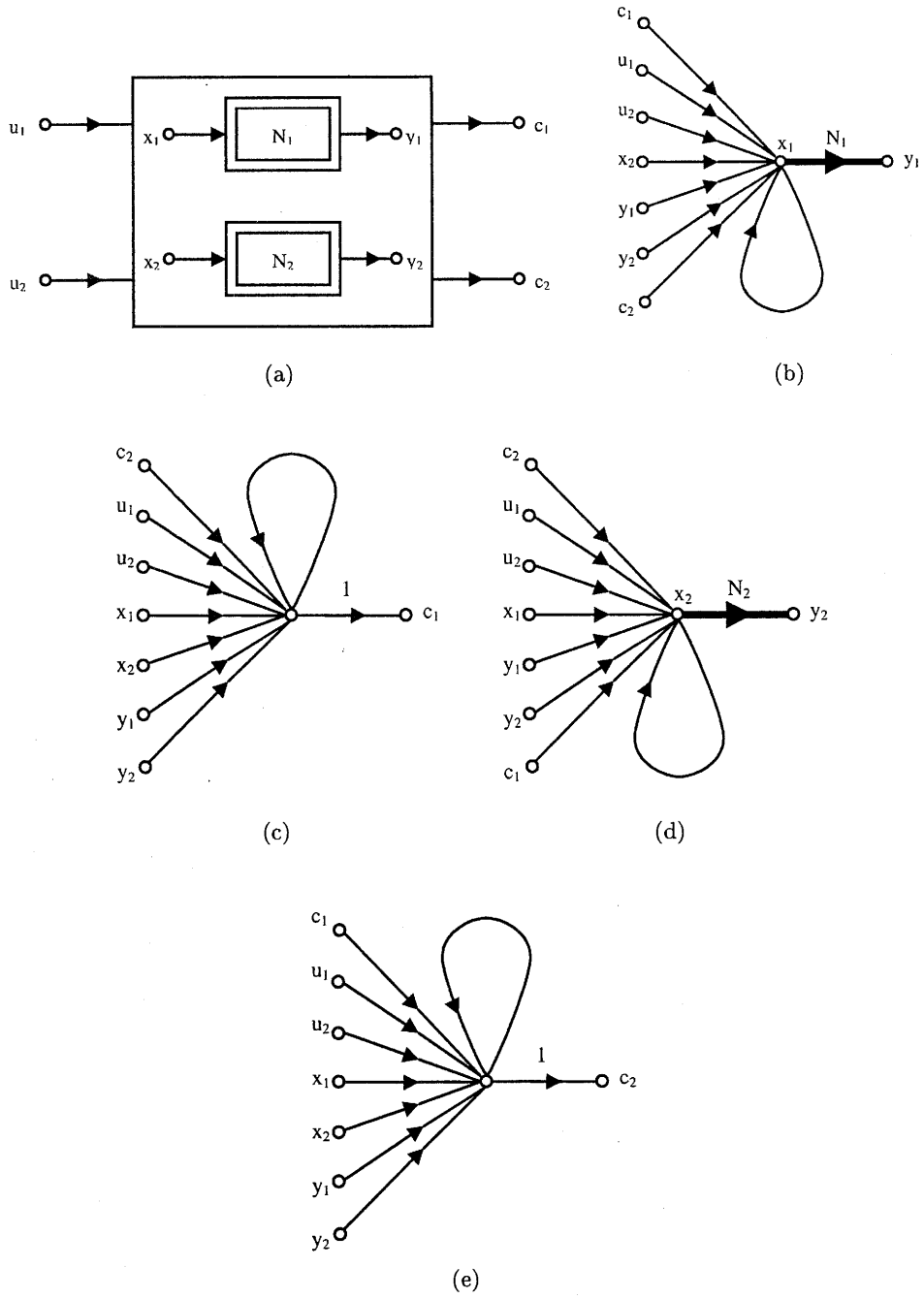

Fig. 1. A most general representation of a 2×2 nonlinear system and relationships between variables.

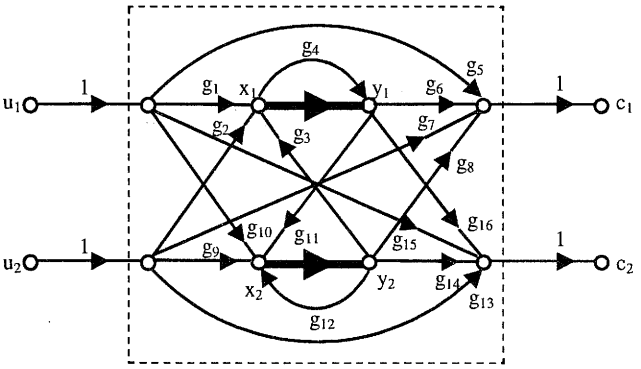

(a)

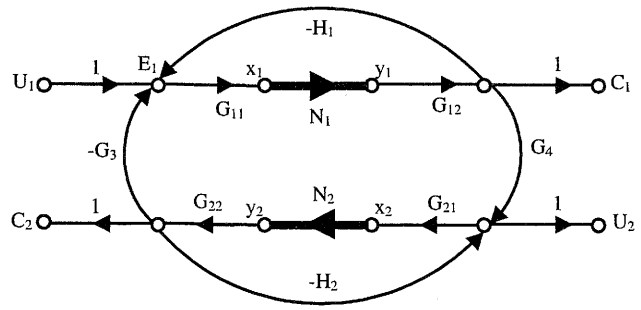

(b)

Fig. 2. A simplified equivalent form of the most general configuration of the 2×2 nonlinear system under consideration.

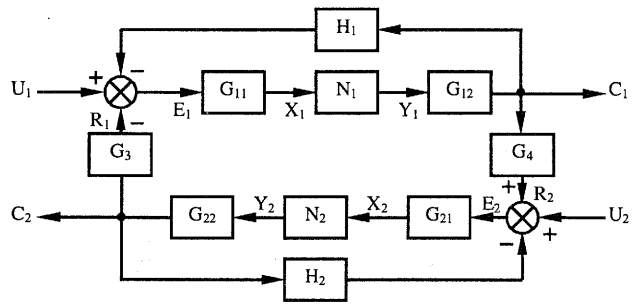

Fig. 3. A most general configuration of the two-dimensional nonlinear system.

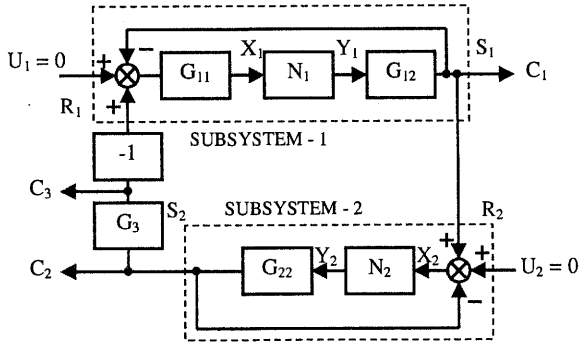

Fig. 4. A most general class of 2×2 nonlinear systems.

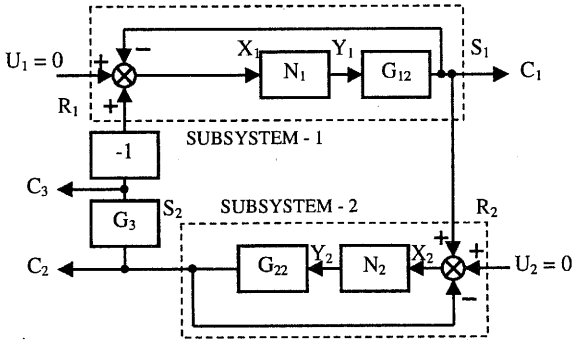

Fig. 5. A general class of 2×2 nonlinear systems.

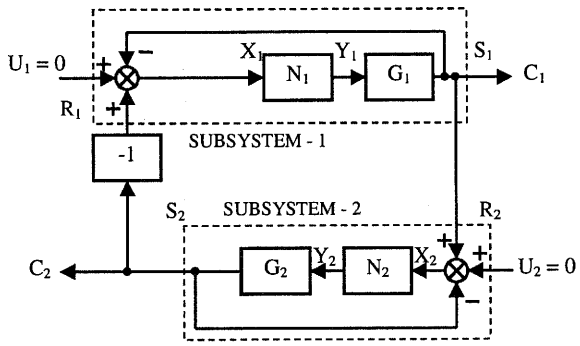

Fig. 6. Another class of 2×2 nonlinear systems.

to Fig. 4, the transfer functions for the linear elements and the outputs C_1, C_2 and C_3 are also transformed even though the same symbols have been retained for convenience. For a higher-dimensional system it becomes practically impossible to analyse the system in terms of its explicit structural form and we have to resort to a matrix formulation. The structure of a most general multidimensional system and the corresponding matrix formulation has been developed in (Patra and Singh, 1994; Patra *et al.*, 1995). The paper analyses the limit cycle behaviour of the system shown in Figs. 4–6 in their autonomous state. In the presentation of the work here, we have sought to increase the complexity of the problem at successive stages, each stage differing from the previous ones in just one respect. This approach is adopted in order to achieve greater clarity of presentation. However, the paper explains in detail application of universal charts for the simplified system of Fig. 6 for clarity. The results for other structures of Figs. 4 and 5 are given in Table 1 for various nonlinearities.

2.1. Limit Cycles in SISO Systems

In general, when a closed-loop system exhibits a sustained oscillation, the signal at any point of the loop is transmitted round the loop to that point with no change in the amplitude and phase. In other words, the system exhibits a self-oscillation when the loop gain is unity and the loop phase shift is $\pm 2n\pi$ (Atherton, 1975), where n is an integer. The equivalent characteristic equation, obtained with the use of DF's of nonlinear elements in the SISO system, satisfies the above two conditions (i.e. the loop gain and phase shift) for the sustained self-oscillations. The characteristic equation deals with complex functions of frequency and hence can be split into two independent equations by separating the real and imaginary parts which can yield the amplitude and frequency of self-oscillations.

2.2. Limit Cycles in Two-Dimensional Systems

Consider a system consisting of two interconnected subsystems as shown in Figs. 4–6. A rigorous analysis of periodic phenomena in such systems is extremely complex. However, if the system exhibits a predominantly single frequency oscillation, and if the loops possess low-pass characteristics, then a simplified analysis based on the first harmonic linearisation approach can be developed along the following lines (Atherton, 1975; Patra, 1986; Patra and Singh, 1996).

2.2.1. The Universal Chart Method for the Analysis of Limit Cycles

Consider the system shown in Fig. 6 in an autonomous state. When such a system exhibits a limit cycle at a frequency ω, then making use of DF's, $N_1(X_1)$ and $N_2(X_2)$, of the nonlinear elements, the characteristic equation in the frequency domain is obtained as

$$1 + N_1(X_1)G_1(j\omega) + N_2(X_2)G_2(j\omega) + 2N_1(X_1)N_2(X_2)G_1(j\omega)G_2(j\omega) = 0$$

Three unknowns X_1, X_2 and ω require three independent equations for their evaluation. By separating the real and imaginary parts of the above equation (after

substituting the linear elements by the corresponding frequency response functions) only two independent equations involving the three unknown quantities can be developed. Therefore the characteristic equation alone is not sufficient for the analysis of limit cycles in such systems. However, replacing the nonlinear elements by the respective DF's, we note that for a possible limit cycle the following conditions must be satisfied for ensuring harmonic balance (Patra, 1986; Patra *et al.*, 1995):

(i) The Phase Condition:

$$\theta_{c_1} + \theta_{c_2} = 180^{\circ} \tag{1}$$

where

$$\theta_{c_1} = \text{Arg}\left[\frac{N_1 G_1(j\omega)}{1 + N_1 G_1(j\omega)}\right]$$

$$\theta_{c_2} = \text{Arg}\left[\frac{N_2 G_2(j\omega)}{1 + N_2 G_2(j\omega)}\right]$$

(ii) The Gain Condition:

$$\frac{C_1\, C_2}{R_1\, R_2} = 1 \tag{2}$$

where

$$\frac{C_1}{R_1} = \left|\frac{N_1 G_1(j\omega)}{1 + N_1 G_1(j\omega)}\right|$$

$$\frac{C_2}{R_2} = \left|\frac{N_2 G_2(j\omega)}{1 + N_2 G_2(j\omega)}\right|$$

(iii) The Amplitude Ratio Condition:

$$\frac{X_2}{R_2} = \left|\frac{1}{1 + N_2 G_2(j\omega)}\right|, \quad R_2 = C_1 = N_1 G_1(j\omega) X_1$$

leading to

$$\frac{X_2}{X_1} = \left|\frac{N_1 G_1(j\omega)}{1 + N_2 G_2(j\omega)}\right| \tag{3}$$

The last condition has been derived from relationships between the system variables. One may use the ratio C_1/R_1 for that purpose instead. So whether the C_1/R_1 or X_1/X_2 ratio is used for the comparison or plotting, is a matter of individual preferences. Our option is to use the latter because of its easy determination from the intersection-point coordinates and at least in some part beacause it seems to be a

more appealing data representation from the system eigenvector concept (Patra *et al.*, 1995; Patra and Singh, 1994).

The method comprises two steps. The first one determines all the possible solutions satisfying only the phase and gain conditions for self-oscillations (cf. eqns. (1) and (2)) and the second one determines possible solutions satisfying only the gain condition and the amplitude ratio condition (cf. eqns. (2) and (3)). The intersections of the possible solutions obtained from the two steps would simultaneously satisfy all the three conditions for the existence of a self-oscillation and therefore yield the desired solutions.

Step 1. Possible solutions satisfying phase and gain conditions.

The phasor diagram shown in Fig. 7 represents the phasors of the subsystems S_1 and S_2 of the system of Fig. 6 (Patra and Singh, 1996). From the triangle ABD of Fig. 7, we have

$$\frac{\sin(180^\circ - \theta_{Lm})}{R_m} = \frac{\sin(\theta_{Lm} - \theta_{cm})}{C_m}$$

or

$$\log \frac{C_m}{R_m} = \frac{\sin(\theta_{L_m} - \theta_{cm})}{\sin \theta_{Lm}}, \quad m = 1, 2 \tag{4}$$

where θ_{Lm} stands for the phase angle between X_m and $C_m = \mathrm{Arg}(G_m(j\omega))$ (assuming that the nonlinear elements involve no phase shift) and θ_{cm} denotes the phase angle between C_m and R_m.

For particular values of θ_{L1} and θ_{L2} that correspond to a specific ω (assumed), a plot of $\log(C_m/R_m)$ versus θ_{cm} can be obtained. We note that for a sustained self-oscillation $\theta_{c1} + \theta_{c2} = 180^\circ$ and $\log(C_1/R_1) = -\log(C_2/R_2)$ (cf. eqns. (1) and (2)).

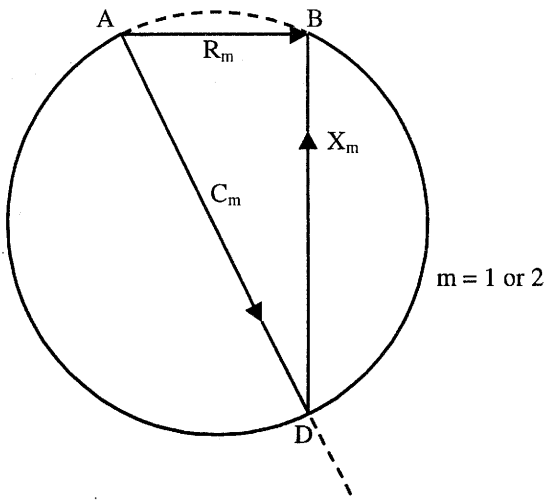

Fig. 7. The phasor diagram for the system of Fig. 6.

Hence possible solutions simultaneously satisfying these conditions can be directly obtained if both the plots ($\log(C_1/R_1)$ vs. θ_{c1} and $\log(C_2/R_2)$ vs. θ_{c2}) are superposed back to back and intersect each other. If no intersection occurs, then no solution exists. This process is repeated for a range of ω and the values of $\log(C_1/R_1) = -\log(C_2/R_2)$ corresponding to the intersections are noted and subsequently a plot of $\log(C_1/R_1)$ vs. ω is obtained.

It is interesting to note that the plot of $\log(C_m/R_m)$ vs. θ_{cm} depends on θ_L and does not depend on any particular characteristic of the system under consideration. Hence two families of such curves can be drawn for various values of θ_{L1} and θ_{L2}. These have been designated as the universal curves (Patra, 1986; Patra and Singh, 1996).

The two sets of curves are superposed on each other in the manner shown in Fig. 8 (cf. Example 1). For each ω, the angles θ_{L1} and θ_{L2} are known and we check for the existence of intersections between the θ_{L1} curve of one set of universal curves with the corresponding θ_{L2} curve of the other set in Fig. 8.

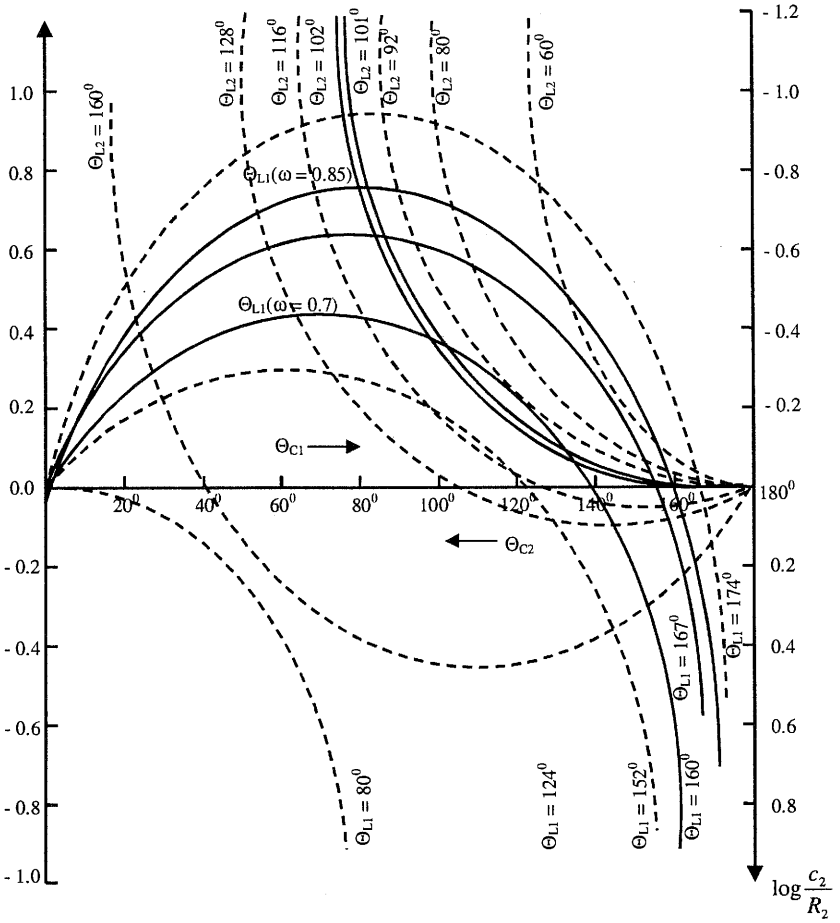

Fig. 8. Superposition of universal curves for the system of Example 1.

Step 2. Possible solutions satisfying the gain and amplitude ratio conditions.

The universal chart (Atherton, 1975; Singh, 1965) provides an elegant and simple method for determining solutions satisfying the gain and amplitude ratio conditions.

The phasor diagram shown in Fig. 7 also yields

$$\log \frac{X_m}{R_m} = \log \frac{\sin \theta_{cm}}{\sin \theta_{Lm}}, \quad m = 1, 2 \tag{5}$$

Hence, for a chosen value of θ_{Lm} and by taking θ_{cm} as a parameter, a plot of $\log(C_m/R_m)$ versus $\log(X_m/R_m)$ can be obtained. This is called the universal chart (Atherton, 1975; Singh, 1965).

Each curve of the universal chart also represents a plot of $\log C_m$ versus $\log X_m$ provided that the origin of the chart is shifted to a point O^1 having coordinates $(-\log R_m, -\log R_m)$ as in Fig. 9. Mathematically, this can be expressed as follows:

$$\log C_m = \log \frac{\sin(\theta_{Lm} - \theta_{cm})}{\sin \theta_{Lm}} + \log R_m, \quad m = 1, 2 \tag{6}$$

$$\log X_m = \log \frac{\sin \theta_{cm}}{\sin \theta_{Lm}} + \log R_m, \quad m = 1, 2 \tag{7}$$

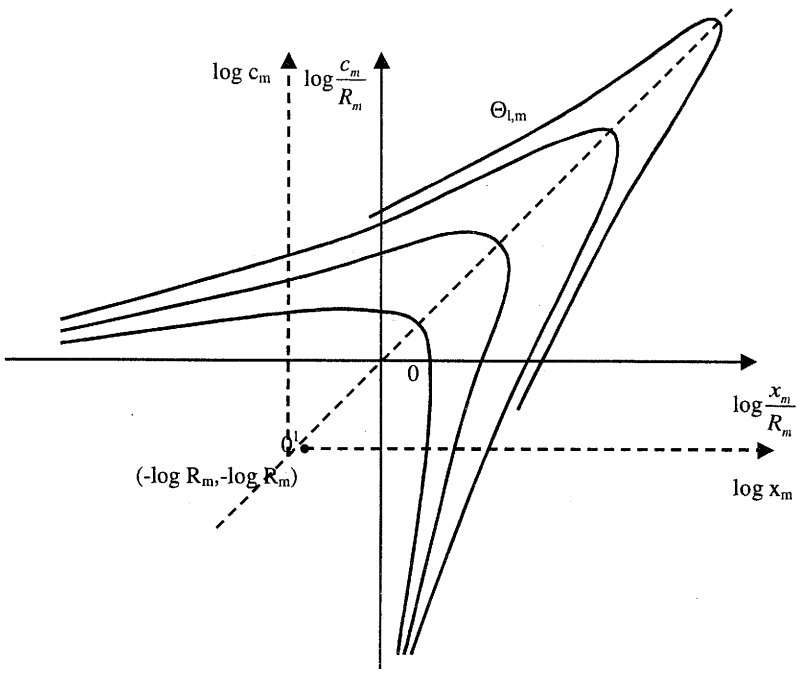

Fig. 9. The universal chart with a shifted origin.

Assuming a frequency ω, a plot of $\log C_m$ versus $\log X_m$ can be obtained for a particular R_m (with θ_{cm} as the parameter). Further, examination of the system of Fig. 6 also leads to

$$\begin{cases} \log C_m = \log Y_m + \log G_m \\ \log Y_m = \log N_m + \log X_m, \quad m = 1,2 \end{cases} \tag{8}$$

The DF's (N_m's) for both the nonlinear subsystems will be given. The plots of $\log Y_m$ versus $\log X_m$ for saturation-type nonlinearities are shown in Fig. 10.

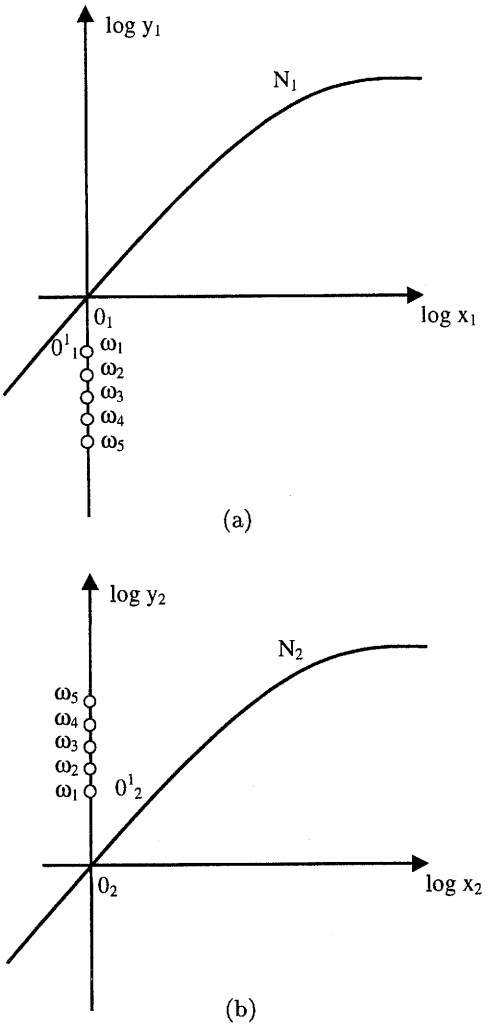

Fig. 10. System characteristics on the universal chart plane.

For a particular assumed ω, a plot of $\log C_m$ versus $\log X_m$ can be obtained at various values of X_m using eqn. (8). Now, we have two sets of $\log C_m$ versus $\log X_m$ plots: the first is found by shifting the origin of the universal chart and the second by shifting the DF plot. If both the plots are superposed on each other, the intersection of the DF plot with that from the shifted universal chart will yield possible values of $\log C_m$ for each chosen value of ω and R_m. For a particular value of ω, by considering various R_m's, $\log C_m$ values can be determined and hence the ratio C_m/R_m. For a limit cycle to occur, R_2 must be equal to C_1 and $R_1 = -C_2$. In view of eqn. (2), the C_1/R_2 value is plotted versus R_1 and the reciprocal of C_2/R_2 is plotted versus $-C_2$. The intersection gives the C_1/R_1 value satisfying the gain and amplitude conditions for the assumed ω.

The whole procedure is repeated for a range of ω and the values of $\log C_1/R_1$ obtained for each ω are plotted. Both the plots of $\log C_1/R_1$ versus ω obtained from Steps 1 and 2 are superimposed and the intersection gives the frequency of a limit cycle satisfying all the three conditions mentioned in eqns. (1)–(3).

Once the frequency of self-oscillations is determined, the amplitudes of other variables of interest can subsequently be determined in a straightforward manner.

The following example is intended to illustrate the procedure outlined above.

Example 1. Consider the system shown in Fig. 6 with $G_1(s) = 2/s(s+1)^2$, $G_2(s) = 1/s(s+4)$, the two nonlinear elements having ideal saturation characteristics with saturation limits $S_1 = 1.5$ and $S_2 = 2.0$, respectively, and the unit linear gain.

The DF's for the two nonlinear elements (N_1 and N_2) are (Atherton, 1975) as follows:

$$\begin{aligned} N_1(X_1) &= \frac{2}{\pi}\left(\sin^{-1}\frac{1.5}{X_1} + \frac{1.5}{X_1}\sqrt{1-(1.5/X_1)^2}\right) \quad \text{for } X_1 > 1.5 \\ N_1(X_2) &= \frac{2}{\pi}\left(\sin^{-1}\frac{2.0}{X_2} + \frac{2.0}{X_2}\sqrt{1-(2.0/X_2)^2}\right) \quad \text{for } X_2 > 2.0 \end{aligned} \tag{9}$$

Step 3. The superposition of the two sets of universal curves is shown in Fig. 8 (for clarity, only a few curves are shown) and the values of $\log(C_1/R_1)$ yielded by the intersection points at several frequencies are read out leading to the plot of $\log(C_1/R_1)$ versus ω shown as curve A in Fig. 12.

Step 4. For the nonlinear characteristics considered in this example the curves N_1 ($\log Y_1$ versus $\log X_1$) and N_2 ($\log Y_2$ versus $\log X_2$) are shown in Figs. 10(a) and (b), respectively, and the origins, $O_m s$, corresponding to several values of ω are also marked in the same figures. The universal chart for the system can be drawn following the procedure outlined in Step 2.

For a typical value of $\omega = 0.775$ and $R_1 = 0.74$, the superposition of the N_1 curve on the universal chart ($\theta_{L1} = 165.55$) is shown in Fig. 11(a) and yields the value of $C_1 = 1.74$ and 2.95. Similary, for $R_2 = 2.95$ at the same frequency the superposition of the N_2 curve on the universal chart ($\theta_{L2} = 101.0$) shown in

Fig. 11(b) yields $C_2 = 0.74$. For several values of R_m, the C_m/R_m ratios were found and plotted as explained earlier. The intersection points give the value of C_1/R_1 for the assumed frequency.

The process is repeated for several values of ω and the corresponding values of $\log(C_1/R_1)$ which satisfy the required gain and amplitude ratio conditions are noted and based on these results a plot of $\log(C_1/R_1)$ versus ω is added as curve B in Fig. 12.

The point of intersection of curves A and B in Fig. 12 yields ω, the frequency of self-oscillation, as 0.7813 rad/sec.

Subsequently, the amplitudes of the other variables of interest are determined as

$$X_1 = 2.997, \quad X_2 = 2.9743, \quad C_1 = 2.9038, \quad C_2 = 0.7345$$

Step 2 of the universal-chart method appears to be somewhat cumbersome at first sight. However, the whole programme has been implemented with the use of MATLAB 4.0 leading to fairly accurate results at the expense of a small amount of computational and graphic work (Table 1). ♦

2.3. The Most General System

Consider the system of Fig. 4. For this, the subsystem S_2 along with G_3 can be considered as one subsystem. We can take for static and memory-less nonlinearities

$$\begin{cases} \theta_{L1} = \text{Angle}\big(G_{11}(j\omega)\big) + \text{Angle}\big(G_{12}(j\omega)\big) \\ \theta_{L2} = \text{Angle}\big(G_{22}(j\omega)\big) + \text{Angle}\big(G_3(j\omega)\big) \end{cases} \tag{10}$$

The subsystem gains are C_1/R_1 and C_3/R_2, respectively. A limit cycle occurs when $C_1 = R_2$ and $C_3 = -R_1$. The steps explained for the analysis of Fig. 6 can be used for this system with these modifications.

The system of Fig. 5 is the same as that of Fig. 4 except for the linear element $G_{11} = 1.0$ here.

Example 2. Consider the system of Fig. 4 with $G_{11}(s) = s+1$, $G_{12}(s) = 2/s(s+1)^3$, $G_{22}(s) = 1/s(s+4)$, $G_3(s) = 1/(s+1)(s+4)$ and the two nonlinear elements having ideal saturation characteristics with saturation limits $S_1 = 1.5$ and $S_2 = 1.0$, respectively, and unit linear gain. The results of the limit cycle analysis are given in Table 1. ♦

Example 3. Consider the system of Fig. 5 with $G_{12} = 2/s(s+1)^2$, $G_{22}(s) = 1/s(s+4)$, $G_3(s) = 1/(s+3)$ and the two nonlinear elements having ideal saturation characteristics with saturation limits $S_1 = 1.5$ and $S_2 = 1.0$, respecively, and unit linear gain. The results of the limit cycle analysis are given in Table 1.

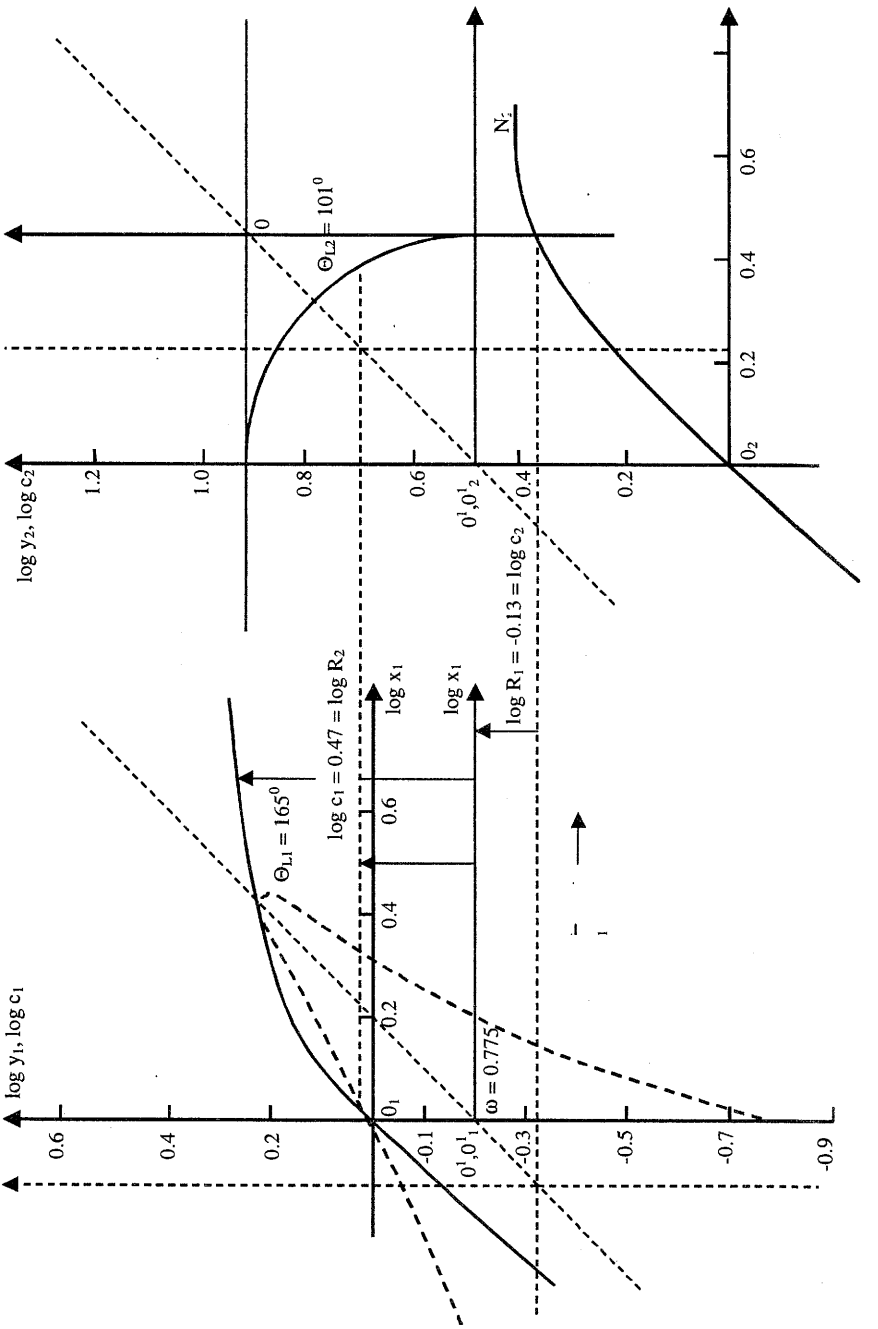

Fig. 11. Superposition of universal chart on N_1 and N_2 curves of Example 1 ($\theta_{L1} = 165.55°$ and $\theta_{L2} = 100.96°$ for $\omega = 0.775$ rad/sec).

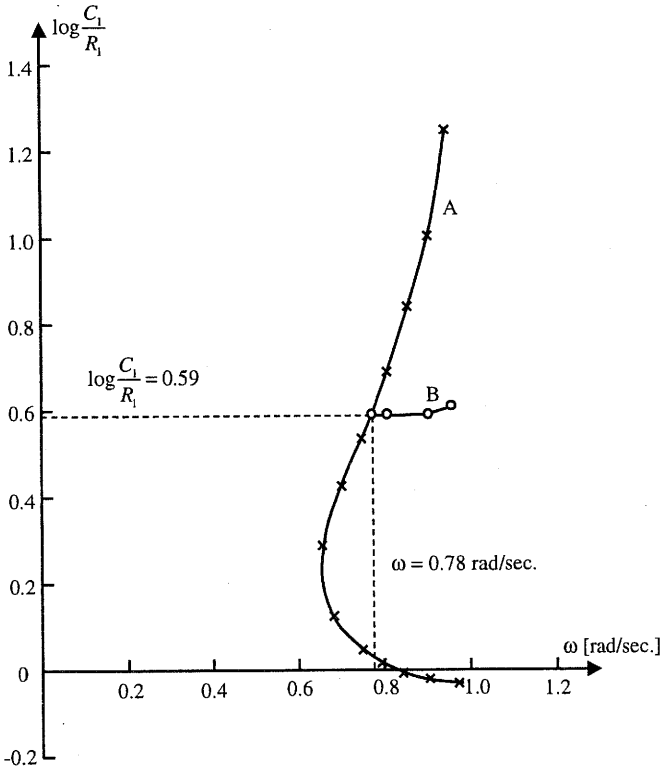

Fig. 12. The solution to the system of Example 1.

Table 1. Results of Examples.

Example	Parameter	Graphical	Digital simul^n	Simulink
1	ω [rad/s]	0.7813	0.7728	0.7854
	C_1	2.9038	2.9559	3.05
	C_2	0.7345	0.7719	0.8
	X_1	2.9973	3.0583	2.99
	X_2	2.9743	3.0684	3.15
2	ω [rad/s]	0.9737	0.9728	0.9779
	C_1	1.1444	1.1645	1.1546
	C_2	0.2754	0.2783	0.2763
	X_1	1.5591	1.5543	1.558
	X_2	1.1839	1.1941	1.1893
3	ω [rad/s]	0.9511	0.9518	0.9533
	C_1	1.8287	1.8158	1.8289
	C_2	0.3111	0.3211	0.3289
	X_1	1.7967	1.7763	1.838
	X_2	1.8811	1.8826	1.8703

3. Digital Simulation

A digital simulation method for the system considered here is similar to the one earlier used by the authors (Patra *et al.*, 1995). The method makes use of an extension of two-dimensional nonlinear systems of the technique adopted by (Subramanian, 1978) for SISO systems. For clarity, the technique is illustrated by application to a specific example.

Example 4. Consider the system of Example 1. A state variable representation for this system in canonic form is shown in Fig. 13. Introduction of samplers at the input and output points of the nonlinear elements and insertion of a gain T (since $TG(z) \simeq G(s)$ for a small T) leads to the equivalent $\mathcal{Z}$-transform representation as shown in Fig. 14, where:

$$\begin{aligned} y_1(nT) &= f_1[x_1(nT)], & y_2(nT) &= f_2[x_2(nT)] \\ x_1(nT) &= r_1(nT) - c_1(nT), & x_2(nT) &= r_2(nT) - c_2(nT) \\ r_1(nT) &= -c_2(nT), & r_2(nT) &= c_1(nT) \end{aligned} \tag{11}$$

and

$$\frac{W_1(z)}{Y_1(z)} = \frac{2z}{z-1}, \quad \frac{W_2(z)}{Y_1(z)} = \frac{-2z}{z-e^{-T}}, \quad \frac{W_3(z)}{Y_1(z)} = \frac{-2zTe^{-T}}{(z-e^{-T})^2}$$

$$\frac{V_1(z)}{Y_2(z)} = \frac{0.25z}{z-1}, \quad \frac{V_2(z)}{Y_2(z)} = \frac{-0.25z}{z-e^{-4T}} \tag{12}$$

Equation (12) leads to the following difference equations:

$$\begin{aligned} w_1(nT) &= 2y_1(nT) + w_1\big([n-1]T\big) \\ w_2(nT) &= -2y_1(nT) + e^{-T}w_2\big([n-1]T\big) \\ w_3(nT) &= -2Te^{-T}y1\big([n-1]T\big) + 2e^{-T}w_3\big([n-1]T\big) - e^{-2T}w_3\big([n-2]T\big) \\ v_1(nT) &= 0.25y_2(nT) + v_1\big([n-1]T\big) \\ v_2(nT) &= -0.25y_2(nT) + e^{-4T}v_2\big([n-1]T\big) \end{aligned} \tag{13}$$

$$c_1(nT) = T\big\{w_1(nT) + w_2(nT) + w_3(nT)\big\}$$

$$c_2(nT) = T\big\{v_1(nT) + v_2(nT)\big\} \tag{14}$$

Equations (11), (13) and (14) define the recurrence relationships for the system variables and can be directly implemented on a digital computer. It should be noted, however, that in the case of simulation the system demands the presence of a low-frequency signal initially. This is the excitation signal used to initiate the oscillation

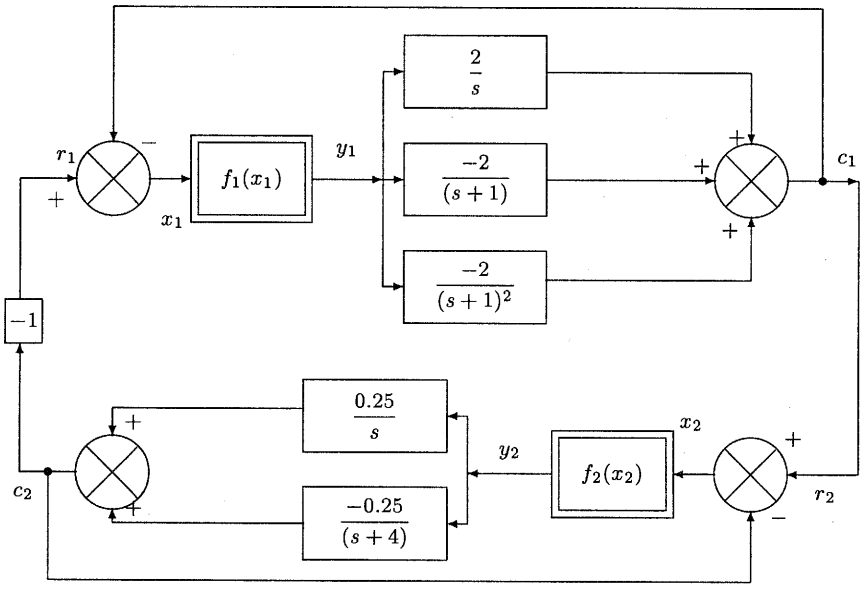

Fig. 13. The state-variable representation in canonic form for the system of Example 4.

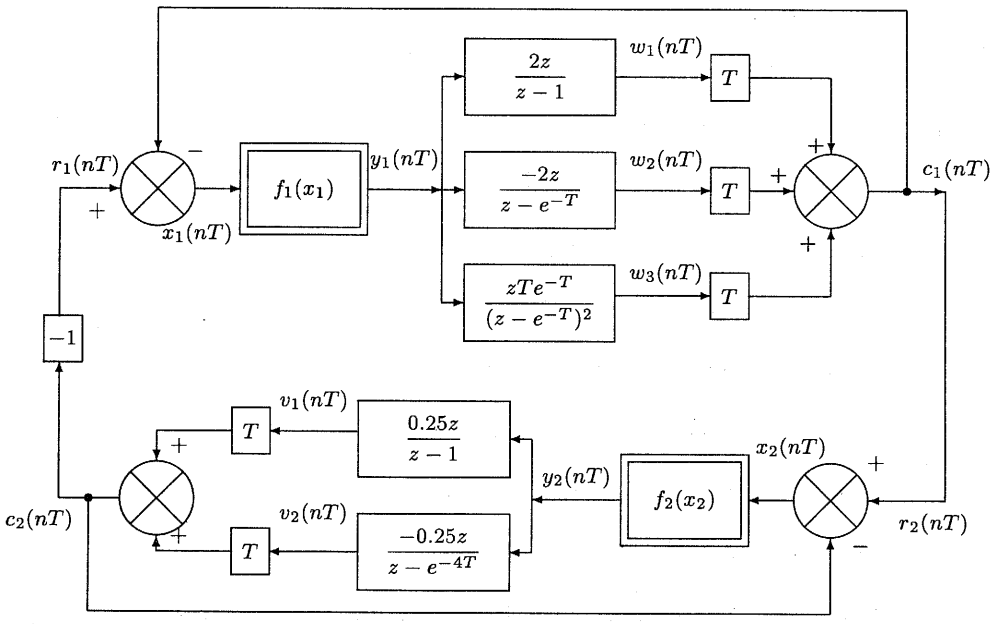

Fig. 14. The digital representation of Fig. 13 in $\mathcal{Z}$-domain.

built up in the system. This technique has been found to yield accurate results with considerable economy in programming and the computing time.

Following the same approach, the limit cycle parameters have been predicted for systems of Examples 2 and 3 too. The results are presented in Table 1 for all the examples.

The proposed method of digital simulation offers the following advantages:

(i) It is based on principles of continuous-time controller approximation and includes therefore an intersampling behaviour of the system.

(ii) The value of the chosen sampling interval is much less ($T = 0.001\,\mathrm{s}$).

(iii) Even for a relatively larger sampling time ($T = 0.01\,\mathrm{sec}$) the results are comparable to the earlier values computed at a small sampling time (verified by an author).

(iv) It is straightforward and works well with any example system.

(v) It is also suitable for multirate sampling.

4. Conclusions

The advantage of the universal-chart method over the other methods is that, being a general method, its use can be extended to systems incorporating nonlinear elements having more general characteristics (including multivalued ones) while the other methods would become exceedingly complex in such cases. In addition, for systems with more complex linear transfer functions and nonlinear characteristics, it would be extremely difficult to formulate and simplify the expressions in the harmonic balance method.

Making use of the universal chart, a graphical method, leading to application of computer graphics has been developed for analysing limit cycles in nonlinear multidimensional systems. The method is particularly elegant for two-dimensional nonlinear systems and can be applied to higher-order systems. This technique can also be extended to the analysis of complex oscillations during the process of signal stabilisation (the dither signal may be fed at u_1 or u_2 of Fig. 6 (Atherton, 1975)). For the system possessing low-pass loop characteristics, the DF analysis provides results of acceptable accuracies as verified from the comparison with results from MATLAB/SIMULINK and digital simulation of the system.

Acknowledgements

The authors wish to thank Professor Y.P. Singh and Professor P.K. Rajgopaplan of the Electrical Engineering Department and Professor S. Subramanian of the Computer Science and Engineering Department, IIT Kharagpur, India, for valuable discussions. This work has been supported by the All-India Council for Technical Education, Govt. of India, under the thrust-area project *Control system including computerised control in industry.*

References

Atherton D.P. (1975): *Nonlinear control engineering-describing function analysis and design.* — London: Van Nostrand Reinhold.

Atherton D.P. and Dorrah H.T. (1980): *A survey on non-linear oscillations.* — Int. J. Contr., Vol.31, No.6, pp.1041–1105.

Nikiforuk P.N. and Wintonyk B.L.M. (1968): *Frequency response analysis of two dimensional nonlinear symmetrical and nonsymmetrical control systems.* — Int. J. Contr., Vol.7, pp.49–62.

Parlos A.G., Henery A.F., Schweppe F.C., Gould L.A. and Lanning D.D. (1988): *Nonlinear multivariable control of nuclear power plants based on the unknown but bounded disturbance model.* — IEEE Trans. Automat. Contr., Vol.AC-38, No.2, pp.130–134.

Patra K.C. (1986): *Analysis of self oscillations and signal stabilisation of two-dimensional nonlinear systems.* — Ph.D. Thesis, I.I.T., Kharagpur, India.

Patra K.C., Pati B.B. and Kacprzyk J. (1995): *Prediction of limit cycles in nonlinear multivariable systems.* — Arch. Contr. Sci., Poland, Vol.4(XL), No.3–4, pp.281–297.

Patra K.C. and Singh Y.P. (1994): *Structural formulation and prediction of limit cycle for multivariable nonlinear system.* — J. IETE, Vol.40, No.5–6, pp.253–260.

Patra K.C. and Singh Y.P. (1996): *Graphical method of prediction of limit cycle for multivariable nonlinear systems.* — IEE Proc. Contr. Th. Appl., Vol.143, No.5, pp.423–428.

Raju G.S. and Josselson R. (1971): *Stability of reactor control systems in coupled core reactors.* — IEEE Trans. Nuclear Sci., Vol.NS-18, pp.388–394.

Singh Y.P. (1965): *Graphical method for finding the closed loop frequency response of nonlinear feedback control system'.* — IEE Proc. Contr. Th. Appl., Vol.112, pp.2165–2170.

Singh Y.P. and Subramanian S. (1980): *Frequency Response Identification of Structure of Nonlinear Systems.* — Proc. IEE, Vol.127, Part D, pp.77–82.

Subramanian S. (1978): *Frequency Response Identification of Nonlinear Systems.* — Ph.D. Thesis, I.I.T., Kharagpur, India.

Received: 5 December 1997
Revised: 14 September 1998